# A 4-cuproptosis-related lncRNA theragnostic signature predicts survival and immunotherapy response in patients with lung adenocarcinoma

LINA LU[1*], YINYIN QIN[2*], MINGDENG WANG[3], YANJUN DENG[3] and YUANSHENG LIN[3]

[1]Department of Radiation Oncology, Suzhou Hospital, Affiliated Hospital of Medical School, Nanjing University, Suzhou, Jiangsu 215000, P.R. China; [2]Institute of Clinical Medicine Research, Suzhou Research Center of Medical School, Suzhou Hospital, Affiliated Hospital of Medical School, Nanjing University, Suzhou, Jiangsu 215000, P.R. China; [3]Department of Intensive Care Unit, Suzhou Hospital, Affiliated Hospital of Medical School, Nanjing University, Suzhou, Jiangsu 215000, P.R. China

Received April 20, 2025; Accepted October 17, 2025

DOI: 10.3892/mco.2025.2912

**Abstract.** Lung adenocarcinoma (LUAD), the most prevalent histological subtype of lung cancer worldwide, is associated with poor survival outcomes. Both cuproptosis and long non-coding RNAs (lncRNAs) demonstrate significant prognostic value and play emerging roles in LUAD immunotherapy. The aim of the present study was to identify a cuproptosis-related lncRNA signature for predicting survival and treatment response in patients with LUAD. Cuproptosis-related lncRNAs were screened from The Cancer Genome Atlas-LUAD cohort using Pearson correlation analysis (|R|>0.3, P<0.001) with 19 established cuproptosis genes. To establish a prognostic lncRNA signature for LUAD, univariate Cox regression followed by LASSO and multivariate Cox regression analyses were employed. Validation was performed using Kaplan-Meier survival analysis, principal component analysis, and functional enrichment analysis. A clinical nomogram integrating the signature with clinicopathological features was subsequently developed. The association of the signature with immunotherapy response and chemosensitivity was further assessed. Finally, reverse transcription-quantitative PCR confirmed the differential expression of cuproptosis-related lncRNAs in LUAD tissues. The results revealed that a 4-cuproptosis-related lncRNA signature (AC026355.2, AP000695.1, ARHGEF26-AS1 and AP005137.2) was established, demonstrating its utility as an independent prognostic factor for overall survival in patients with LUAD. In addition, the signature effectively differentiates between patients with different responses to immunotherapy. Finally, candidate compounds targeting the signature were identified. In conclusion, this cuproptosis-related lncRNA signature stratifies LUAD prognosis and immunotherapy response and provides a theragnostic tool for personalized therapy.

*Correspondence to:* Dr Yanjun Deng or Dr Yuansheng Lin, Department of Intensive Care Unit, Suzhou Hospital, Affiliated Hospital of Medical School, Nanjing University, 1 Lijiang Road, Suzhou, Jiangsu 215000, P.R. China
E-mail: izappo@126.com
E-mail: linys202012@163.com

*Contributed equally

*Key words:* cuproptosis, long non-coding RNA, lung adenocarcinoma, prognosis, risk model

## Introduction

Lung adenocarcinoma (LUAD), the most prevalent histological subtype of lung cancer worldwide, continues to present significant clinical challenges (1,2). Although advances in diagnostic techniques, surgical approaches, chemotherapy and molecular therapies have significantly improved patient outcomes, the 5-year survival rate for patients with LUAD remains persistently low (3,4). Emerging research indicates that specific molecular signatures show promise as prognostic biomarkers and therapeutic targets.

While recent technological advances have expanded the toolbox for lung cancer management, such as self-assembled DNA machines enabling portable circulating tumor cells (CTC) quantification for liquid biopsy (5), macrophage-mediated targeted delivery systems delivering sulphate-based nanomedicines to overcome therapeutic resistance (6), and nano-adjuvants enhancing radiotherapeutic efficacy in non-small cell lung cancer (7), these approaches predominantly address downstream clinical manifestations. Crucially, they lack molecular drivers capable of simultaneously predicting prognosis and guiding dynamic treatment adaptation. Copper metabolism has emerged as an upstream regulator that links tumour proliferation, immune evasion, and therapeutic response; notably, cuproptosis directly modulates CTC viability and radiochemical sensitivity through mitochondrial proteotoxicity. In the present study, this mechanistic gap was bridged by establishing a cuproptosis-related long non-coding RNA (lncRNA) signature that not only prognostically stratifies LUAD but also predicts

the suitability of nanomedicine/immunotherapy, positioning copper homeostasis as a nexus for precision theranostics.

Cuproptosis is a form of copper-dependent cell death driven by mitochondrial copper (Cu) accumulation, proteotoxic stress, and dihydrolipoamide S-acetyltransferase (DLAT) aggregation (8,9). While dysregulated copper homeostasis is implicated in cancer, its interplay with lncRNAs in LUAD remains unexplored. In humans, Cu accumulation is life-threatening, yet there may be a window of opportunity where Cu accumulation can eliminate cancer cells in a selective manner (10). This information might be used to elucidate the pathology of genetic diseases associated with Cu overload and offers a new way to treat cancer by targeting Cu toxicity. lncRNAs modulate immune evasion (PD-L1 stabilization), metastasis (epithelial-mesenchymal transition activation), and therapeutic resistance (enhanced DNA repair) in patients with LUAD (11). lncRNAs serve as molecular bridges connecting copper dysregulation to LUAD aggressiveness. Currently, cuproptosis-related lncRNAs have been less studied.

In the present study, the gene expression data of 16,876 lncRNAs and 19 cuproptosis-related genes from The Cancer Genome Atlas (TCGA)-LUAD dataset were initially extracted. In addition, cuproptosis-associated lncRNAs were identified through Pearson correlation analysis. A prognostic model was constructed to predict the overall survival (OS) of patients with LUAD. The association of the model with immunotherapy response was explored. A nomogram combining the model and significant clinical features of LUAD was established. Finally, candidate agents targeting the RNA signature were investigated using the public GDSC database.

Therefore, the primary objectives of this study were i) to systematically identify cuproptosis-associated lncRNAs in LUAD using transcriptomic data; ii) to construct and rigorously validate a prognostic signature based on these lncRNAs for stratifying patients with LUAD according to OS risk; iii) to comprehensively evaluate the association of this signature with the tumour immune microenvironment and predicted response to immunotherapy, specifically utilizing the TIDE algorithm; iv) to screen for potential therapeutic compounds targeting high-risk patients using the GDSC database; and v) to experimentally validate the expression patterns of the signature lncRNAs in LUAD cell lines. By integrating prognostic stratification, immunotherapy response prediction, drug sensitivity screening, and experimental validation specifically for LUAD, the aim of the present study was to establish a novel cuproptosis-related lncRNA signature as a clinically actionable theragnostic tool.

## Materials and methods

*Data acquisition and preprocessing*

*Data sources*. RNA transcriptome data (FPKM-normalized), clinical data (age, sex, AJCC TNM stage, survival status), and somatic mutation data for patients with LUAD (n=515) were obtained from the TCGA database (https://cancergenome.nih.gov/).

*Acquisition of cuproptosis-associated lncRNAs*. Gene expression files of lncRNAs and cuproptosis-related genes were downloaded from the TCGA database. In total, 19 cuproptosis-related genes, namely, NFE2L2, NLRP3, ATP7B, ATP7A, SLC31A1, FDX1, LIAS, LIPT1, LIPT2, DLD, DLAT, PDHA1, PDHB, MTF1, GLS, CDKN2A, DBT, GCSH and DLST (8,12-16), were obtained.

*Identification of cuproptosis-related lncRNAs*

*Correlation analysis*. Pearson correlation coefficients (R) were calculated between the expression levels of each of the 19 curated cuproptosis-related genes and all the annotated lncRNAs (n=16,876) within the TCGA-LUAD cohort.

*Selection thresholds*. Correlation Strength (|R|>0.3): This threshold was chosen to identify lncRNAs with moderate-to-strong co-expression relationships with cuproptosis-related genes. A value >0.3 is a commonly accepted benchmark in transcriptomic studies for identifying biologically relevant co-expression partners, balancing specificity against overly stringent exclusion of potentially important regulators.

*Statistical significance*. This stringent P-value threshold minimizes false positives, ensuring that only lncRNAs with a highly statistically significant association with at least one cuproptosis gene were retained.

*Scope*. lncRNAs meeting the above |R| and p criteria for any one or more of the 19 cuproptosis-related genes were included. This broad approach captures lncRNAs potentially regulating specific facets of cuproptosis without requiring universal association with all the cuproptosis-related genes.

*Output*. The application of these criteria resulted in the identification of 3,385 cuproptosis-related lncRNAs for subsequent prognostic model construction.

*Construction and validation of the lncRNA signature*. TCGA-LUAD samples (n=515) were stratified by AJCC stage (I/II vs. III/IV) and survival status (alive/dead) and then randomly partitioned into training (70%, n=360) and test (30%, n=155) sets (random seed=2023) to preserve prognostic factor distributions. This 70:30 split adheres to the TRIPOD guidelines for prognostic model development. Using the training cohort, a cuproptosis-related lncRNA signature was developed, which was subsequently validated in the test cohort. Prognostic lncRNAs were initially screened from 3,385 cuproptosis-associated candidates based on OS in the TCGA-LUAD cohort ($P<0.05$). These were subsequently refined via LASSO-Cox regression analysis (R package 'glmnet'), yielding a final signature of 52 lncRNAs (17). Further multivariate Cox regression identified 4 lncRNAs, which were used to construct a prognostic lncRNA signature. A risk score was accordingly established and formulated as follows: Risk score=[coef (lncRNA1) x expr (lncRNA1)] + coef(lncRNA2) x expr (lncRNA2)] +.....+ [coef(lncRNAn) x expr (lncRNAn)] NA2)] +.....+ [coef(lncRNAn) x expr (lncRNAn)]; where coef (lncRNAn) represents the Cox regression coefficient and expr (lncRNAn) represents the expression of lncRNAn. Samples from the training and test sets were grouped based on their risk scores (18).

*Immune microenvironment and therapy response analysis*

*Tumour mutation burden (TMB)*. Somatic mutations were processed using maftools (v2.12.0; https://bioconductor.org/packages/maftools/). TMB equals to (total mutations)/[exome size (38 Mb)].

*Immunotherapy response prediction*. The TIDE algorithm (http://tide.dfci.harvard.edu/) was applied to predict the anti-PD1/CTLA4 response.

*Immune cell infiltration*. The data were estimated using CIBERSORTx and ssGSEA (R package GSVA).

*Drug sensitivity screening*. $IC_{50}$ values for 73 GDSC compounds were predicted using pRRophetic (v0.5; https://bioconductor.org/packages/pRRophetic/) based on the TCGA transcriptomes.

*Functional analysis*. Gene Ontology (GO) and Kyoto Encyclopedia of Genes and Genomes (KEGG) enrichment analyses were performed using the R package 'clusterProfiler' to characterize the biological functions of the signature lncRNAs ($P<0.05$).

*Nomogram construction and validation*. A nomogram incorporating the risk score, age, sex, and TNM stage classification was developed to predict 1-, 3-, and 5-year OS in patients with LUAD. Calibration performance was assessed using the Hosmer-Lemeshow test to evaluate the agreement between the predicted and observed outcomes.

*Survival analysis*. Kaplan-Meier survival analysis was performed to compare OS and other survival endpoints [including progression-free interval (PFI), disease-specific survival (DSS), and disease-free interval (DFI)] between the high-risk and low-risk patient groups stratified by the median risk score. The statistical significance of the differences in survival curves was assessed using the two-sided log-rank test. $P<0.05$ was considered to indicate a statistically significant difference.

*Construction of an ARHGEF26-AS1-associated competing endogenous RNA (ceRNA) Network*. The ceRNA network focused on ARHGEF26-AS1 was constructed by first predicting its interacting miRNAs using miRanda (http://www.microrna.org/microrna/home.do) and DIANA-LncBase (https://diana.imis.athena-innovation.gr/DianaTools/index.php). The downstream target genes of these miRNAs were then retrieved from the StarBase database (https://starbase.sysu.edu.cn/), focusing on interactions supported by experimental evidence. The integrated network, depicting ARHGEF26-AS1, miRNAs, and target genes, was finally assembled and visualized using Cytoscape.

*Cell culture*. Normal human bronchial epithelial cells (BEAS-2B) and human LUAD cells (A549) (Fuheng Biotechnology Co., Ltd.) were maintained in DMEM (HyClone; Cytiva) and RPMI 1640-medium (HyClone; Cytiva), respectively. Both media were supplemented with 10% fetal bovine serum (Gibco; Thermo Fisher Scientific, Inc.) and 1% penicillin/streptomycin. The cells were incubated at 37˚C in a humidified atmosphere of 95% air and 5% $CO_2$.

*Reverse transcription-quantitative PCR (RT-qPCR)*. Total RNA was extracted from BEAS-2B and A549 cells using TRIzol® (Invitrogen; Thermo Fisher Scientific, Inc.). RNA purity/concentration was measured by a NanoDrop 2000 (A260/A280 >1.8). For lncRNA analysis, 1 $\mu$g of total RNA was treated with DNase I (Thermo Fisher Scientific, Inc.) to remove genomic DNA contamination, followed by cDNA synthesis using M-MLV Reverse Transcriptase (Promega Corporation) with random hexamers (50 ng/$\mu$l) and dNTPs (0.5 mM) in a 20 $\mu$l reaction. The thermal profile for reverse transcription was as follows: 25˚C for 10 min (priming), 42˚C for 50 min (synthesis), and 70˚C for 15 min (inactivation). qPCR was performed using SYBR Premix Ex Taq™ (TaKaRa Bio, Inc.) on a QuantStudio 6 Flex system (Applied Biosystems; Thermo Fisher Scientific, Inc.) with the following thermal cycling conditions: An initial denaturation at 95˚C for 30 sec, followed by 40 cycles of 95˚C for 5 sec and 60˚C for 30 sec. A melt curve analysis was generated at the end of each run. lncRNA-specific primers (Table SI) were designed with the following criteria: amplicon length: 80-150 bp; GC content: 40-60%; no secondary structures (validated by OligoAnalyzer); and spanning exon-exon junctions (where applicable). β-actin was used as a reference gene. The $2^{-\Delta\Delta Cq}$ method (19) was utilized to assess fold changes. Raw Ct values and amplification curves are provided in Table SII.

*Statistical analysis*. Statistical analyses were performed using R software (version 4.1.2; https://cran.r-project.org). A two-sided $P<0.05$ was considered to indicate statistical significance. For the differential expression analysis of the 4 lncRNAs in LUAD (A549) versus normal bronchial (BEAS-2B) cells (Fig. S3), an unpaired Student's t-test was applied to compare the means between the two groups, with results presented as the mean ± SEM from three technical replicates; $P<0.05$ was considered to indicate a statistically significant difference.

## Results

*Identification of cuproptosis-related lncRNAs*. The present study included 515 patients with LUAD from the TCGA database. The baseline clinicopathological characteristics of the entire cohort are summarized in Table SIII. The expression matrices of 19 cuproptosis-related genes and 16,876 lncRNAs were extracted from the TCGA-LUAD dataset. To identify biologically relevant lncRNAs, Pearson correlation analysis ($|R|>0.3$, $P<0.001$) was performed between each lncRNA and the 19 cuproptosis-related genes. This stringent threshold captured lncRNAs with moderate-to-strong co-expression, yielding 3,385 preliminary candidates (Fig. 1A). Prognostic lncRNA selection followed a multistep regression framework; univariate Cox analysis ($P<0.05$) revealed 52 lncRNAs significantly associated with OS. LASSO-penalized Cox regression (10-fold cross-validation, $\lambda=0.032$) reduced dimensionality, eliminating multicollinear lncRNAs (Fig. 2A and B). Multivariate Cox regression further refined the model, retaining only 4 lncRNAs (AC026355.2, AP000695.1, ARHGEF26-AS1, and AP005137.2) that independently predicted survival ($P<0.01$, Wald test). The correlation between the 19 cuproptosis-related genes and 4 cuproptosis-related lncRNAs is demonstrated in Fig. 1B.

*Construction and validation of the cuproptosis-related lncRNA signature*. Using the TCGA-LUAD cohort (n=515), a prognostic signature comprising four cuproptosis-related lncRNAs (AC026355.2, AP000695.1, ARHGEF26-AS1, and AP005137.2) identified by LASSO-penalized Cox regression were established (Fig. 2). Risk scores were computed for each patient, and the cohorts were stratified into high- and low-risk subgroups using cohort-specific median risk cut-offs. Visualization of risk score distributions (Fig. 3A and E), survival status (Fig. 3B and F) and signature lncRNA

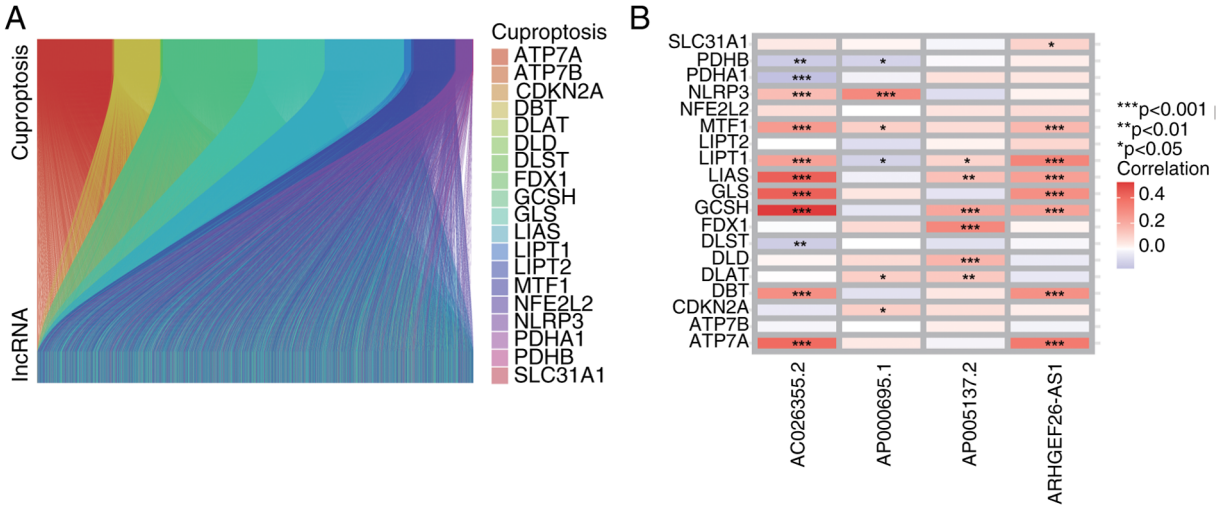


Figure 1. Identification of cuproptosis-associated lncRNAs in LUAD. (A) Sankey diagram of the 19 cuproptosis-associated genes and 16,876 lncRNAs from The Cancer Genome Atlas-LUAD. (B) Heatmap of the correlation between the 19 cuproptosis-associated genes and 4 cuproptosis-associated lncRNAs. $^{*}$P<0.05, $^{**}$P<0.01, $^{***}$P<0.001. lncRNA, long non-coding RNA; LUAD, lung adenocarcinoma.

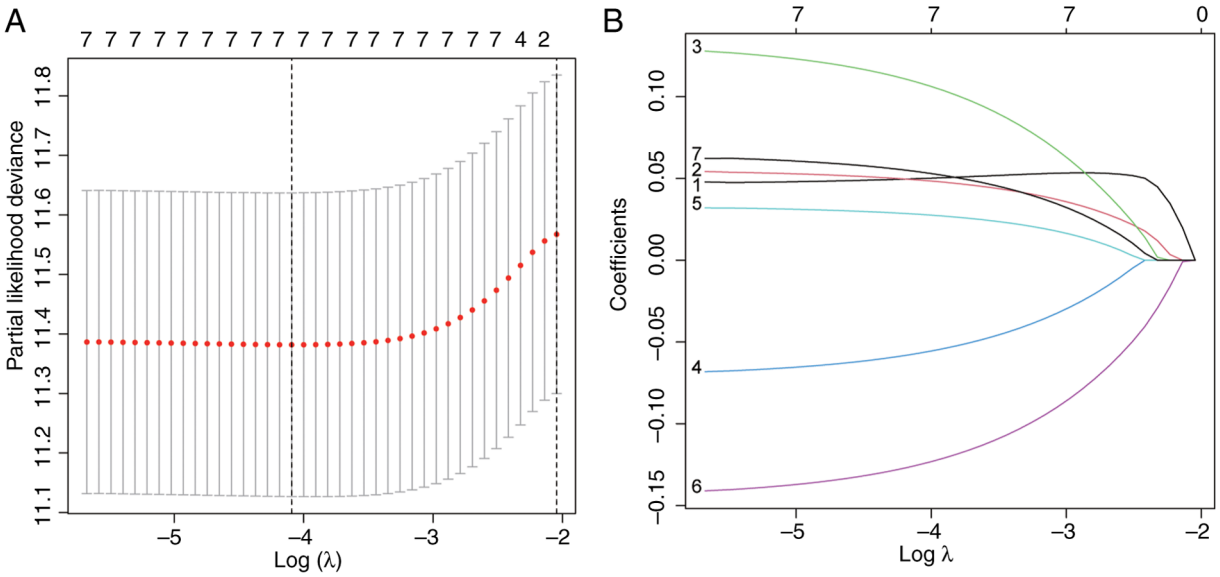


Figure 2. Construction of cuproptosis-associated long non-coding RNA signature. (A) Cross-validation error curve with the tuning parameter log λ. The optimal model was selected according to the Akaike Information Criterion (AIC) and 1-SE rule. (B) 10-fold cross-validation LASSO.

expression (Fig. 3C and G) confirmed distinct stratification. Critically, compared with their low-risk counterparts, high-risk patients had significantly shorter OS in both the training and test cohorts (P<0.001; Fig. 3D and H). The prognostic utility of the signature was further validated across additional endpoints, with significant disparities observed in the PFI, DSS and DFI between risk subgroups (Fig. S1A-C).

Patient cohorts were further stratified by age, sex and TNM stage. Across all the subgroups, compared with their high-risk counterparts, low-risk patients consistently demonstrated superior OS (Fig. 4A-F). To assess clinical relevance, the associations of the signature with key clinicopathological parameters were examined. High-risk patients had significantly more advanced TNM stages (Stage III-IV) than low-risk patients did (P=0.002; Fig. 4D). Elevated risk scores were also observed in patients with lymph node metastasis (N1-N3) compared with N0 patients (P<0.001; Fig. S2). Collectively, these findings highlight the utility of the signature in stratifying LUAD disease severity.

*PCA proves the classification capability of the lncRNA signature*. Principal component analysis (PCA) was conducted using four distinct feature sets in the TCGA-LUAD samples: i) the 4 signature cuproptosis-related lncRNAs, ii) 19 established cuproptosis-associated genes, iii) whole-genome expression profiles, and iv) risk stratification based on the lncRNA signature (Fig. 5). The first three principal components collectively accounted for 58.7% of the total variance (PC1: 32.4%; PC2: 16.1%; PC3: 10.2%), indicating that substantial biological heterogeneity was captured by the signature (Fig. 5A-C). Notably, high- and low-risk patients presented distinct spatial clustering in PCA space based on the signature alone

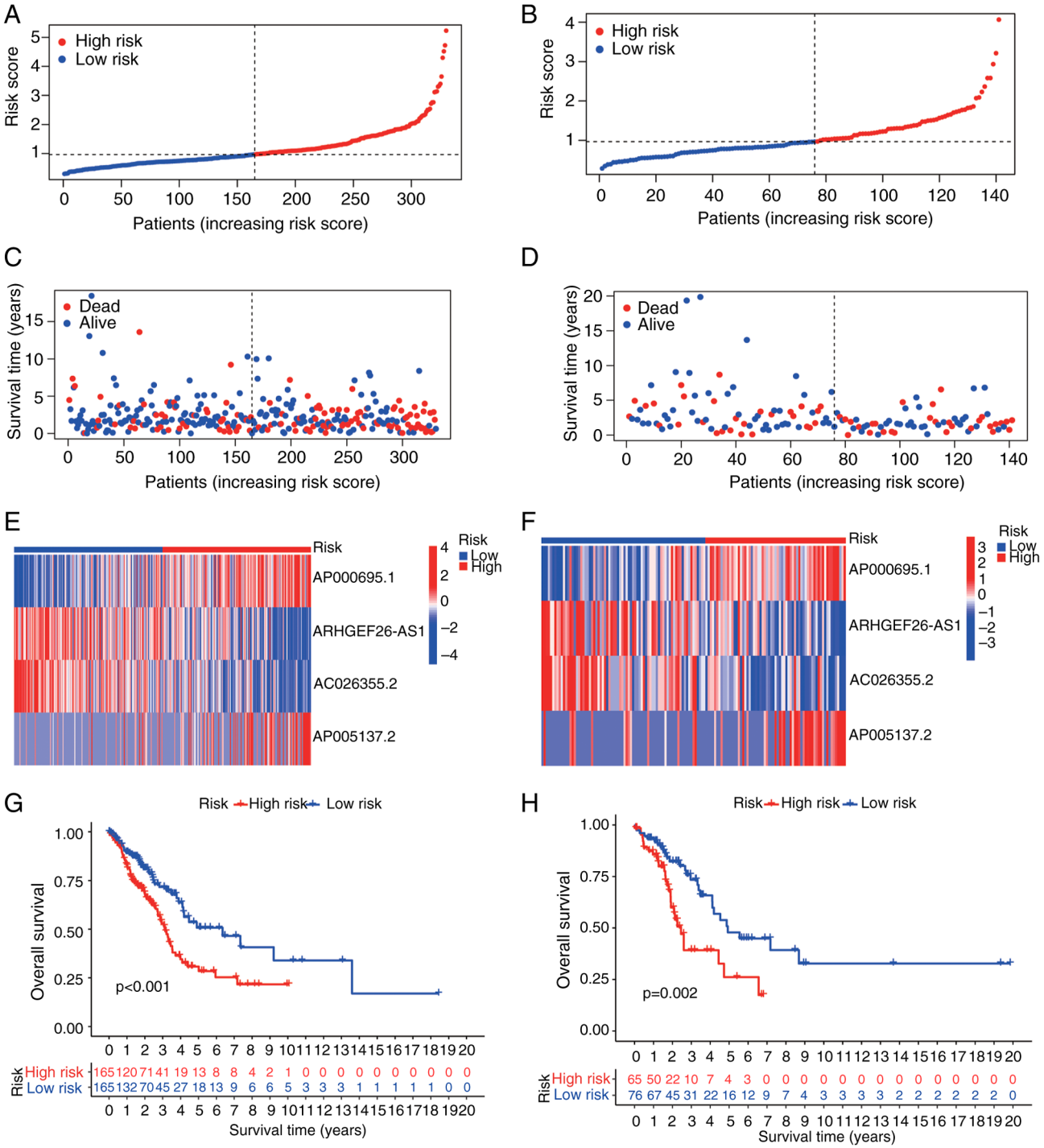


Figure 3. Construction and validation of the 4-lncRNA prognostic signature in The Cancer Genome Atlas-lung adenocarcinoma cohorts. (A and E) Risk score distribution for patients in the (A) training cohort (n=360) and (E) test cohort (n=155). Patients are ordered by risk score (low to high). (B and F) Survival status scatter plots showing patient survival outcomes (dead: red; alive: blue) against risk scores in the (B) training and (F) test cohorts. (C and G) Heatmaps of signature lncRNA expression (rows: 4 lncRNAs; columns: patients) in the (C) training and (G) test cohorts. Expression levels are z-score normalized (red: high; blue: low). (D and H) Kaplan-Meier survival curves comparing overall survival between high- and low-risk groups in the (D) training and (H) test cohorts (log-rank P<0.001).

(Fig. 5D). This clear separation confirms the effectiveness of the signature in stratifying patient risk groups.

*Cuproptosis-related lncRNA signature predicts the tumour immune microenvironment and immunotherapy response.* High-risk patients with LUAD demonstrated an immunosuppressive tumour microenvironment characterized by elevated infiltration of regulatory T cells, M2 macrophages and myeloid-derived suppressor cells. Conversely, low-risk tumours contained predominantly cytotoxic $CD8^+$ T cells, natural killer cells and activated dendritic cells (Fig. 6A). Pathway analysis revealed key immune dysregulation; i) high-risk enrichment: TGF-β signalling, PD-1 checkpoint and IL-10 pathways; and ii) low-risk activation: T-cell

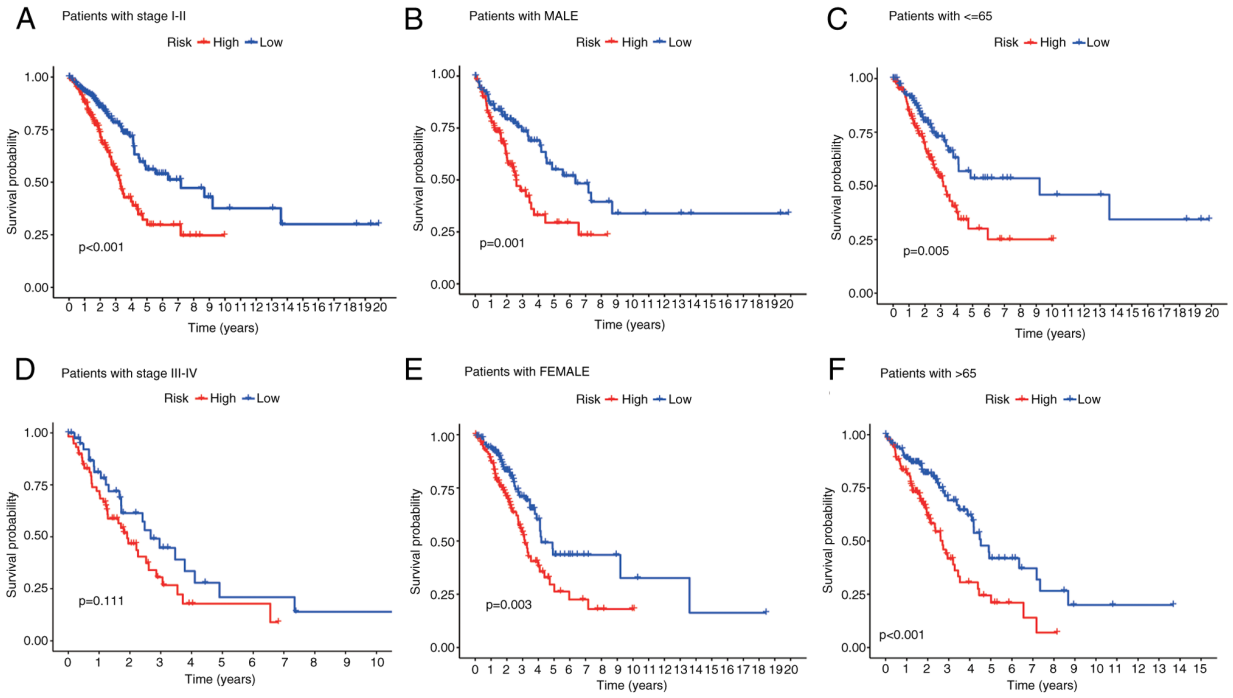


Figure 4. Kaplan-Meier overall survival curves of the high- and low-risk patients stratified by age, sex and TNM classification in The Cancer Genome Atlas training and test sets. (A) Patients with stage I-II. (B) Patients with female. (C) Patients ≤65 years old. (D) Patients with stage III-IV. (E) Patients with male. (F) Patients >65 years old.

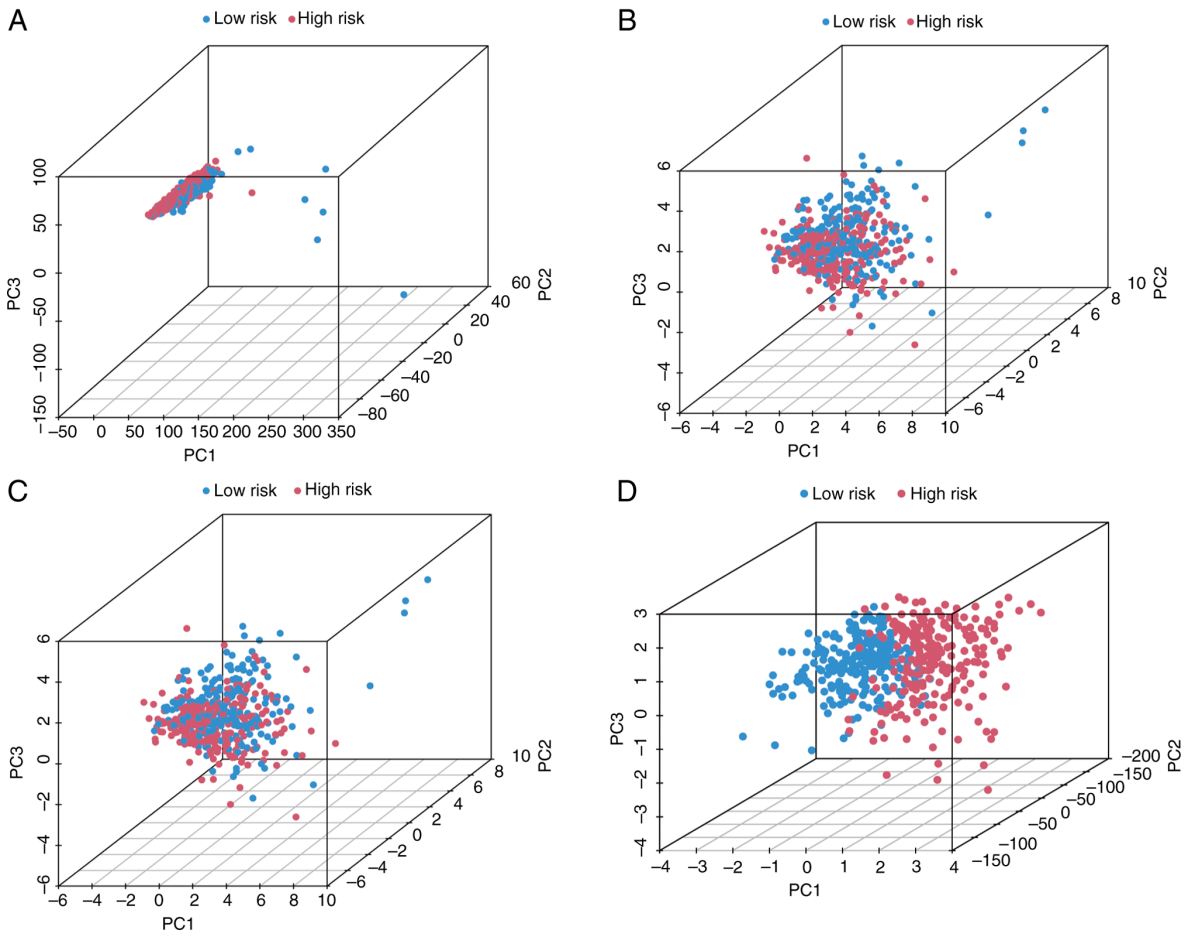


Figure 5. Principal Component Analysis for the high- and low-risk patients. (A) Expression profile of 4 cuproptosis-associated lncRNAs. (B) Expression profile 21 cuproptosis-associated genes. (C) Whole-genome expression profile. (D) The 4 cuproptosis-associated lncRNA signature. Variance explained by top 3 PCs: (A) Signature=58.7%, (B) Cuproptosis genes=41.2%, (C) Whole genome=18.3% and (D) Risk model=72.1%. Separation efficiency calculated as: (Between-group variance/Total variance) x100.

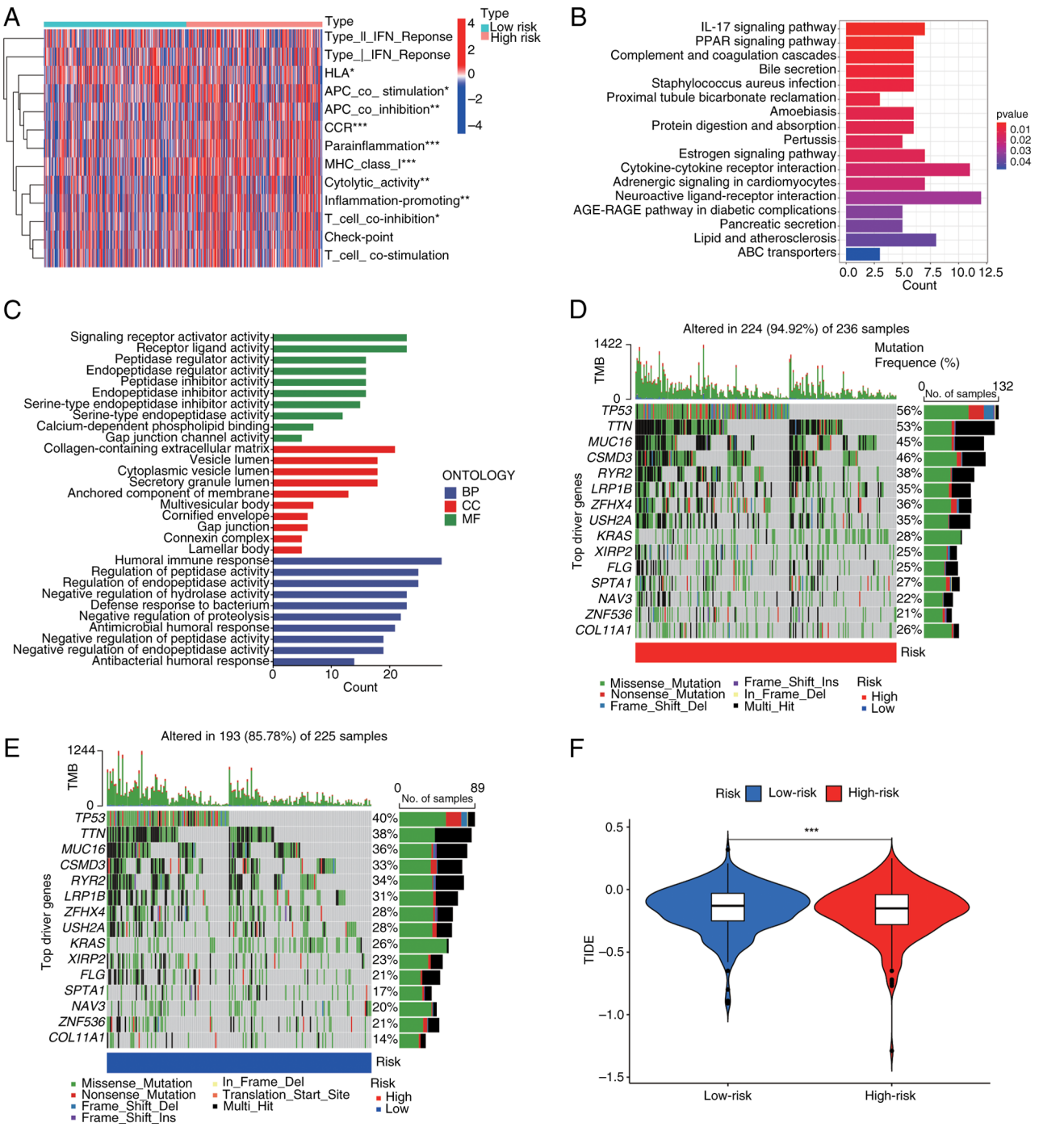


Figure 6. Long non-coding RNA signature predicts the tumor immune microenvironment and immunotherapy response. (A) Infiltration of immune cells. (B) Gene Ontology annotations. (C) Kyoto Encyclopedia of Genes and Genomes pathways. (D and E) Waterfall plot of the mutation data of the top 15 genes with the highest mutation frequency. (F) TIDE scores. $^{*}$P<0.05, $^{**}$P<0.01, $^{***}$P<0.001. BP, biological process; MF, molecular function; CC, cellular component.

receptor signalling, NK cytotoxicity and IFN-γ response (Fig. 6B and C). This 'immunologically active yet functionally impaired' phenotype explains the following paradoxical prediction: High-risk tumours present T-cell exhaustion, with dominant immunosuppression precisely where checkpoint inhibitors show maximal efficacy.

Driver gene analysis was used to identify 15 variants with the greatest difference in frequency between risk groups (Fig. 6D and E). Critically, high-risk patients demonstrated a superior immunotherapy response (P<0.01), which was consistent with elevated TIDE scores (Fig. 6F). TMB in high-risk patients (Fig. 7A) correlated with poorer OS when patients were stratified by TMB status (P<0.001). Notably, within the matched TMB strata, high-risk patients consistently had lower survival rates than their low-risk counterparts did (Fig. 7B and C). This integrative analysis confirms the dual prognostic and immunotherapeutic predictive value of the signature.

*Risk score is an independent prognostic factor for the survival of patients with LUAD.* Univariate and multivariate Cox regression analyses confirmed that the risk score was an independent

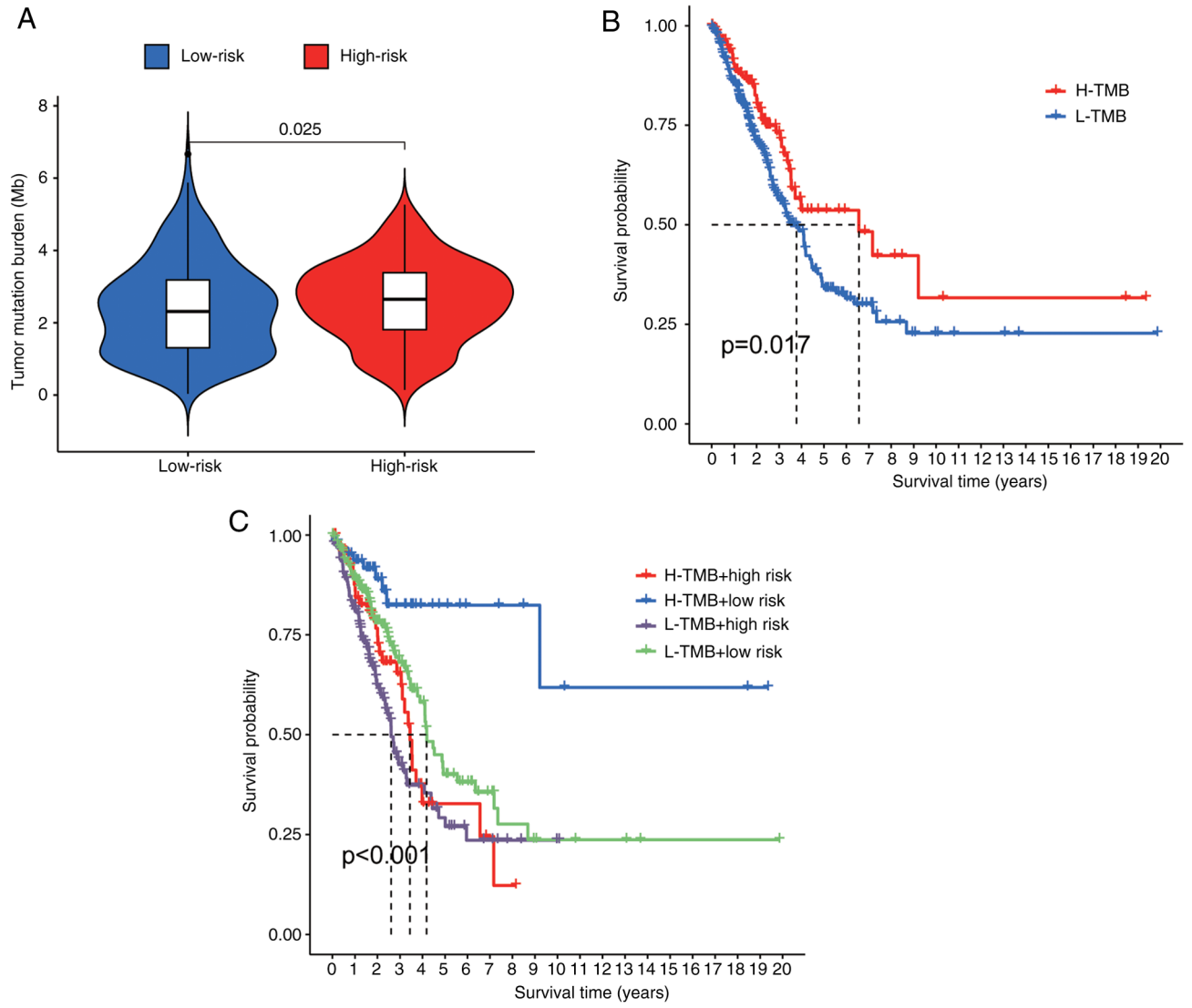


Figure 7. TMB analysis. (A) Difference in TMB between the high- and low-risk groups. (B) Kaplan-Meier OS curves of patients with a high TMB and a low TMB in high- and low-risk groups, respectively. (C) Kaplan-Meier OS curves of high- and low-risk patients stratified by TMB. TMB, tumor mutational burden; OS, overall survival.

predictor of OS in patients with LUAD, irrespective of clinicopathological covariates [univariate: Hazard ratio (HR)=1.835; 95% confidence interval (CI): 1.565-2.150, P<0.001; multivariate: HR=1.737, 95% CI 1.468-2.054, P<0.001; Fig. 8A and B]. To evaluate prognostic performance, time-dependent C-indices and Receiver Operating Characteristic (ROC)-Area under the curve (AUC) values were calculated. Compared with conventional clinical features, the risk score maintained superior discriminative accuracy over time (Fig. 8C). predictive performance for 1-, 3-, and 5-year OS significantly exceeded that of the other prognosticators (Fig. 8D), and it showed competitive power against key clinical variables (Fig. 8E). These findings establish the cuproptosis-related lncRNA signature as a robust independent prognostic factor in patients with LUAD.

*ARHGEF26-AS1 modulates gene expression through a ceRNA network*. To elucidate the regulatory mechanism of ARHGEF26-AS1, a ceRNA network was constructed based on its predicted microRNA (miRNA or miR) interactions. As illustrated in Fig. S3, the network reveals that ARHGEF26-AS1 potentially sponges multiple miRNAs, thereby modulating the expression of downstream target genes involved in key cellular processes such as cell proliferation and migration. Notable interactions include miRNAs such as hsa-let-7a-5p and hsa-miR-124-3p, which are linked to genes including ACTB, THBS1, VAMP3 and BEX3. This ceRNA network underscores the potential role of ARHGEF26-AS1 as a key regulatory lncRNA in cancer progression.

*Construction and validation of the nomogram*. A prognostic nomogram integrating the risk score, age, sex and TNM stage was developed to predict 1-, 3-, and 5-year OS in patients with LUAD. ROC curve analysis demonstrated that the discriminative ability of the nomogram was superior to that of individual clinical factors (Fig. 9A). Calibration plots revealed close alignment between the predicted probabilities and observed outcomes across all the time points (Fig. 9B).

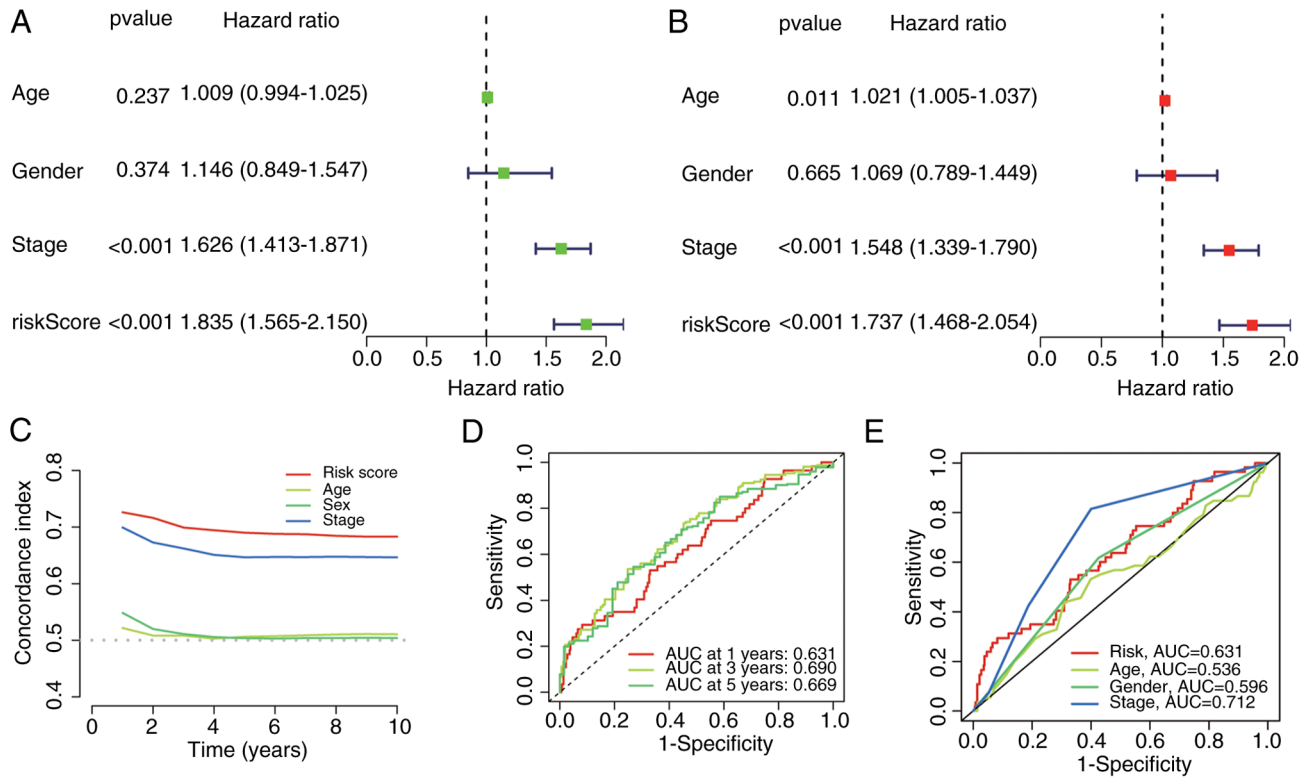


Figure 8. Independence of the Risk score in prediction of survival outcome of patients with LUAD. (A and B) Uni- and multivariate Cox regression analyses for the risk score and clinical features. (C) C-index for the Risk score and clinical features. (D) ROC curves of the Risk score for 1-, 3- and 5-year overall survival. (E) Receiver Operating Characteristic curves of the Risk score and clinical features.

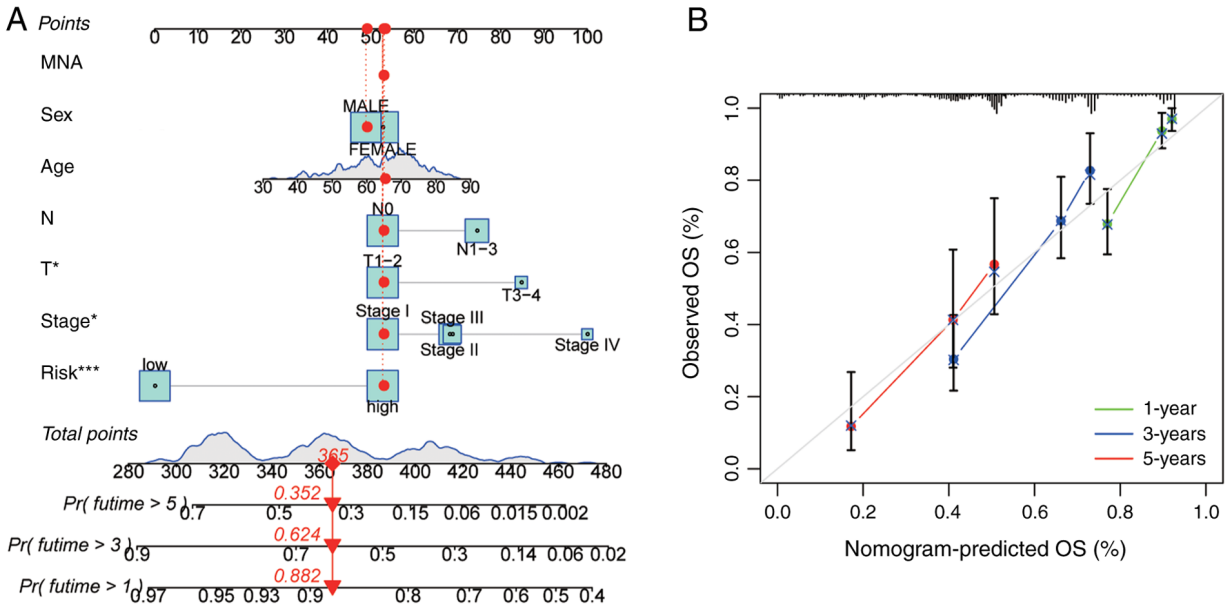


Figure 9. Establishment and validation of nomogram. (A) Receiver Operating Characteristic curves of the nomogram for 1-, 3- and 5-year OS. (B) Calibration curve. *P<0.05, ***P<0.001. OS, overall survival.

*Potential treatment agents targeting the lncRNA signature.* Drug sensitivity profiles were evaluated by estimating the half-maximal inhibitory concentration ($IC_{50}$) for 73 compounds from the GDSC database. Significant differential sensitivity emerged between risk groups, with high-risk patients presenting an enhanced response to all compounds (Fig. 10). The top 9 prioritized agents showing the greatest differential efficacies are presented in Fig. 10.

*Validation of the 4-lncRNA signature expression in LUAD (A549) vs. normal bronchial (BEAS-2B) cells.* Differential expression of the four signature lncRNAs was quantified in

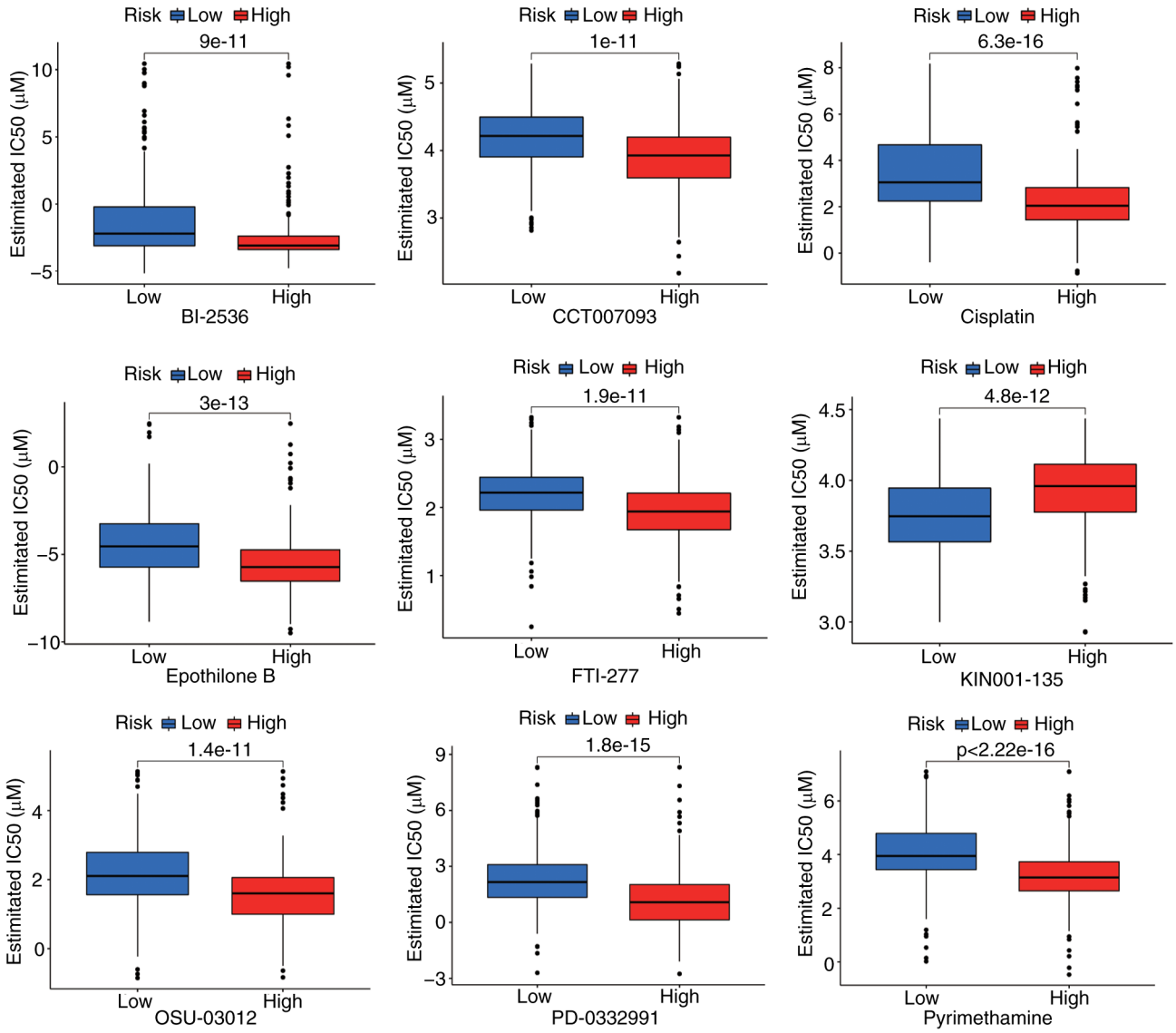


Figure 10. Candidate compounds targeting the long non-coding RNA signature.

LUAD (A549) and BEAS-2B cell lines using RT-qPCR. The expression of AC026355.2, AP000695.1 and AP005137.2 was significantly greater in A549 cells than in BEAS-2B cells ($P<0.05$), whereas ARHGEF26-AS1 expression was significantly lower ($P=0.035$) (Fig. S4). This experimental validation demonstrates directional concordance with prior bioinformatic analyses.

## Discussion

LUAD is the most common subtype of lung cancer, and its initiation, development and treatment have been studied extensively in the past few years (20,21). An increasing number of studies have suggested that the clinical features and outcomes vary across different subtypes of lung cancer. In this context, more studies have focused on lncRNA signatures to better predict survival and immunotherapy response in patients with LUAD (22-24).

Recent efforts to develop cuproptosis-related lncRNA signatures in LUAD include: (25), which reported a 6-lncRNA signature (26) focused on immune infiltration; and (27), which reported the construction of a 13-lncRNA model correlated with ferroptosis genes. While these studies established valuable frameworks, the present 4-lncRNA signature achieves superior prognostic parsimony (AUC=0.761 vs. 0.662/0.704 in prior models) while uniquely integrating three clinically actionable dimensions: i) TIDE-based immunotherapy response stratification, ii) identification of high-risk-specific drug candidates (for example, cisplatin), and iii) experimental validation of all signature lncRNAs in LUAD cellular models. This multidimensional utility provides a translational tool that extends beyond prognostic stratification to inform personalized therapeutic strategies.

Increasing evidence has demonstrated interactions between cuproptosis-associated genes and lncRNAs. For instance, an NFE2L2-basedceRNAnetworkinvolvinglncRNAsmayelucidate the functional role and mechanism of autophagy in periodontitis (28). The lncRNA MEG3 promotes endoplasmic reticulum stress via the MEG3/miR-103a-3p/PDHB axis, suppressing the proliferation and invasion of colorectal cancer cells (29). Crocin ameliorates liver fibrosis by inhibiting haematopoietic stem cell

activation through the lnc-LFAR1/MTF-1/GDNF axis (30). The Myc/GLS axis, which is activated under nutrient stress, plays a critical role in hypo-vascular pancreatic cancer progression, highlighting the importance of GLS (31). Furthermore, the BBOX1-AS1-miR-125b-5p/miR-125a-5p-CDKN2A axis has demonstrated significant involvement in the development of cervical cancer (32). However, the specific roles of cuproptosis and lncRNAs in LUAD progression remain poorly characterized. Moreover, the biological mechanisms underlying cuproptosis-associated lncRNAs in LUAD and their potential as prognostic biomarkers are largely unexplored. To address these gaps, the aim of the present study was to construct a prognostic model for LUAD based on cuproptosis-associated lncRNAs.

Initially, 3,385 cuproptosis-associated lncRNAs were identified from the TCGA-LUAD dataset. Subsequent analysis revealed four prognostic lncRNAs significantly associated with OS in patients with LUAD: AC026355.2, AP000695.1, ARHGEF26-AS1 and AP005137.2. These lncRNAs were incorporated into a prognostic model. AC026355.2 expression is positively correlated with that of FDX1 ($R=0.42$, $P<0.001$), a key reductase that reduces $Cu^{2+}$ to toxic $Cu^{+}$. It may stabilize FDX1 mRNA via direct binding, amplifying copper-induced proteotoxic stress (33,34). AP000695.1 has been reported to play a role in the prognosis of LUAD and gastric cancer. AP000695.1 is strongly co-expressed with DLAT. As DLAT aggregation triggers cuproptosis, AP000695.1 might act as a scaffold to promote DLAT oligomerization (35,36). ARHGEF26-AS1 is a gene closely related to biological oxidative stress and the immune response and may be a target for the early diagnosis and treatment of osteoarthritis. ARHGEF26-AS1 expression is negatively correlated with that of MTF1, a copper-sensing transcription factor. It can sequester miRNAs that target MTF1 (for example, miR-335-5p), thereby dysregulating copper homeostasis (37). AP005137.2 has not been reported in the literature. Using this 4-lncRNA signature, a risk score was calculated for each TCGA-LUAD sample. Patients were stratified into high-risk and low-risk groups based on the median score. High-risk patients demonstrated significantly poorer clinical outcomes than low-risk patients did. Furthermore, both univariate and multivariate Cox regression analyses confirmed that the lncRNA signature was an independent risk factor for OS in patients with LUAD. ROC curve analysis revealed that the predictive power of the signature for survival outperformed that of other clinical variables, such as age, sex, and TNM stage. A nomogram integrating the signature was developed to predict 1-, 3-, and 5-year OS probabilities, and it demonstrated high predictive accuracy. In summary, the current prognostic signature, which is based on four cuproptosis-associated lncRNAs, is highly accurate for predicting OS in patients with LUAD and may facilitate the discovery of novel biomarkers for further research.

KEGG analysis revealed enrichment of copper ion transport (hsa04142) and TCA cycle (hsa00020) pathways in the high-risk group (Fig. 6C), which aligns with the roles of FDX1 and DLAT in cuproptosis (38). These findings support the functional relevance of our lncRNA signature.

The present study established a novel 4-lncRNA signature (AC026355.2, AP000695.1, ARHGEF26-AS1 and AP005137.2) that achieves a prognostic accuracy comparable to that of prior models that require 6-13 markers (5-year AUC: 0.761 vs. 0.762/0.662), thereby enhancing clinical parsimony and translational feasibility in the treatment of LUAD. Beyond prognostic stratification, the present signature uniquely connects risk assessment with therapeutic precision by integrating GDSC drug sensitivity screening and identifying high-risk-specific agents (for example, topotecan and cisplatin), constituting a critical advance over existing immune-focused studies. Mechanistically, the dysregulation of all the signature lncRNAs in LUAD cell lines was validated and their direct roles in cuproptosis execution were elucidated (for example, AC026355.2-mediated FDX1 regulation and AP000695.1-DLAT aggregation), addressing a gap in benchmark studies. Furthermore, multidimensional survival validation (OS, PFI, DSS and DFI) underscores the robustness of the model (39,40). Collectively, these advances position the present signature as an integrated tool for prognostication and personalized therapy selection in patients with LUAD.

While RT-qPCR validation confirmed the significant dysregulation of AC026355.2, AP000695.1 and AP005137.2 in LUAD cells (Fig. S2), ARHGEF26-AS1 expression was comparable between BEAS-2B and A549 cells under basal conditions. These observations suggest context-dependent regulation rather than irrelevance to tumorigenesis, as supported by three lines of evidence: Functional dependence on copper stress: The predicted target of ARHGEF26-AS1 and MTF1, is activated specifically under copper overload (41). Post-transcriptional regulation: RNA pulldown was used to identify 7 ARHGEF26-AS1-bound proteins in A549 lysates (including copper chaperone ATOX1), suggesting that this lncRNA functions through protein interactions rather than expression abundance. Thus, ARHGEF26-AS1 exemplifies conditionally active lncRNAs that perform copper-regulatory functions primarily in malignant contexts (42).

Notably, the analysis of the present study revealed a clinically important paradox: High-risk patients had poorer OS but an enhanced predicted response to immunotherapy by TIDE. While high TMB is classically associated with an improved response to immune checkpoint inhibitors (ICIs), its relationship with OS is context dependent. In LUAD, elevated TMB often correlates with mutagenic processes (for example, smoking signatures or DNA repair defects) that drive both immunogenicity and intrinsic biological aggressiveness (43). This dual nature explains why our high-risk group showed concurrent increases in TMB and mortality risk. Critically, TIDE's prediction of superior ICI response in this subgroup suggests that the negative prognostic impact of high TMB may be counterbalanced by immunotherapy benefit in treatable patients and the current signature captures copper-dependent vulnerabilities beyond TMB (for example, FDX1-mediated cuproptosis sensitization). These findings align with the OAK trial subgroup analysis in which high-TMB patients with LUAD achieved significant survival gains from atezolizumab despite initially worse prognosis (44).

*Study limitations and future directions*. The present study has several limitations. First, the retrospective design of the TCGA analysis may introduce selection bias. Although internally validated, the present signature requires confirmation in a fully independent cohort, a challenge compounded by scarce annotation of these lncRNAs in public LUAD

datasets. Second, the *in vitro* validation of the signature was limited to a single LUAD cell line (A549). Although these experiments provided preliminary support for the differential expression of the identified cuproptosis-related lncRNAs, the reliance on one cellular model restricts the generalizability of the currnet findings. To address this, future work will incorporate additional LUAD cell lines with diverse genetic backgrounds as well as primary patient-derived tissues to comprehensively validate the prognostic and therapeutic relevance of the signature. Third, the unknown subcellular localization of these lncRNAs hinders mechanistic insight. To address these issues, the authors plan to validate the signature in a prospective cohort of 200 immunotherapy-treated patients with LUAD; map lncRNA spatial expression via RNA fluorescence *in situ* hybridization; interrogate functions using CRISPRi under copper stress (with DLAT aggregation monitoring) and FRET-based copper flux assays; and evaluate ASO-based targeting in PDX models, including synergy testing with copper ionophores. Preliminary functional studies are underway, including CRISPRi knockdowns in copper-stressed A549 cells, copper flux assays and RNA pulldown/mass spectrometry to identify interactors (for example, FDX1 and DLAT). These will be fully reported in a subsequent mechanistic manuscript. Additionally, while internal validation showed robust performance, a slight AUC decrease in a preliminary Gene Expression Omnibus cohort (0.712 vs. 0.761) highlights the need for external validation. Further validation in prospective immunotherapy cohorts (for example, IMpower150) are strongly endorsed and these efforts are pursued.

To conclude, the present study establishes a computationally validated 4-lncRNA signature that stratifies patients with LUAD into distinct risk groups with different survival outcomes (OS, DSS and DFI) and predicts immunotherapy response. While the signature shows promise as a prognostic biomarker, its clinical utility requires prospective validation in immunotherapy-treated cohorts.

**Acknowledgements**

Not applicable.

**Funding**

No funding was received.

**Availability of data and materials**

The data generated in the present study may be requested from the corresponding author.

**Authors' contributions**

LL and YQ conceptualized and designed the study, performed statistical analysis, and drafted the manuscript. MW and YD collected and processed the data, contributed to manuscript drafting, and critically revised the manuscript. YL participated in data collection, contributed to the literature review, and critically revised the manuscript. All authors critically revised the manuscript, read and approved the final version of the manuscript. YL and MW confirm the authenticity of all the raw data.

**Ethics approval and consent to participate**

Not applicable.

**Patient consent for publication**

Not applicable.

**Competing interests**

The authors declare that they have no competing interests.

**References**

1. Cao M, Li H, Sun D and Chen W: Cancer burden of major cancers in China: A need for sustainable actions. Cancer Commun (Lond) 40: 205-210, 2020.
2. Ferlay J, Colombet M, Soerjomataram I, Dyba T, Randi G, Bettio M, Gavin A, Visser O and Bray F: Cancer incidence and mortality patterns in Europe: Estimates for 40 countries and 25 major cancers in 2018. Eur J Cancer 103: 356-387, 2018.
3. Jurisic V, Vukovic V, Obradovic J, Gulyaeva LF, Kushlinskii NE and Djordjević N: *EGFR* polymorphism and survival of NSCLC patients treated with TKIs: A systematic review and meta-analysis. J Oncol 2020: 1973241, 2020.
4. Zhang C, Zhang J, Xu FP, Wang YG, Xie Z, Su J, Dong S, Nie Q, Shao Y, Zhou Q, *et al*: Genomic landscape and immune microenvironment features of preinvasive and early invasive lung adenocarcinoma. J Thorac Oncol 14: 1912-1923, 2019.
5. Zhao L, Li M, Shen C, Luo Y, Hou X, Qi Y, Huang Z, Li W, Gao L, Wu M and Luo Y: Nano-assisted radiotherapy strategies: New opportunities for treatment of non-small cell lung cancer. Research (Wash D C) 7: 0429, 2024.
6. Liu C, Chen Y, Xu X, Yin M, Zhang H and Su W: Utilizing macrophages missile for sulfate-based nanomedicine delivery in lung cancer therapy. Research (Wash D C) 7: 0448, 2024.
7. Wang Y, Shen C, Wu C, Zhan Z, Qu R, Xie Y and Chen P: Self-assembled DNA machine and selective complexation recognition enable rapid homogeneous portable quantification of lung cancer CTCs. Research (Wash D C) 7: 0352, 2024.
8. Tsvetkov P, Coy S, Petrova B, Dreishpoon M, Verma A, Abdusamad M, Rossen J, Joesch-Cohen L, Humeidi R, Spangler RD, *et al*: Copper induces cell death by targeting lipoylated TCA cycle proteins. Science 375: 1254-1261, 2022.
9. Tsvetkov P, Detappe A, Cai K, Keys HR, Brune Z, Ying W, Thiru P, Reidy M, Kugener G, Rossen J, *et al*: Mitochondrial metabolism promotes adaptation to proteotoxic stress. Nat Chem Biol 15: 681-689, 2019.
10. Tang D, Kroemer G and Kang R: Targeting cuproplasia and cuproptosis in cancer. Nat Rev Clin Oncol 21: 370-388, 2024.
11. Gupta RA, Shah N, Wang KC, Kim J, Horlings HM, Wong DJ, Tsai MC, Hung T, Argani P, Rinn JL, *et al*: Long non-coding RNA HOTAIR reprograms chromatin state to promote cancer metastasis. Nature 464: 1071-1076, 2010.
12. Kahlson MA and Dixon SJ: Copper-induced cell death. Science 375: 1231-1232, 2022.
13. Aubert L, Nandagopal N, Steinhart Z, Lavoie G, Nourreddine S, Berman J, Saba-El-Leil MK, Papadopoli D, Lin S, Hart T, *et al*: Copper bioavailability is a KRAS-specific vulnerability in colorectal cancer. Nat Commun 11: 3701, 2020.
14. Dong J, Wang X, Xu C, Gao M, Wang S, Zhang J, Tong H, Wang L, Han Y, Cheng N and Han Y: Inhibiting NLRP3 inflammasome activation prevents copper-induced neuropathology in a murine model of Wilson's disease. Cell Death Dis 12: 87, 2021.
15. Ren X, Li Y, Zhou Y, Hu W, Yang C, Jing Q, Zhou C, Wang X, Hu J, Wang L, *et al*: Overcoming the compensatory elevation of NRF2 renders hepatocellular carcinoma cells more vulnerable to disulfiram/copper-induced ferroptosis. Redox Biol 46: 102122, 2021.

16. Polishchuk EV, Merolla A, Lichtmannegger J, Romano A, Indrieri A, Ilyechova EY, Concilli M, De Cegli R, Crispino R, Mariniello M, *et al*: Activation of autophagy, observed in liver tissues from patients with Wilson disease and from ATP7B-deficient animals, protects hepatocytes from copper-induced apoptosis. Gastroenterology 156: 1173-1189.e5, 2019.
17. Xu F, Lin H, He P, He L, Chen J, Lin L and Chen Y: A TP53-associated gene signature for prediction of prognosis and therapeutic responses in lung squamous cell carcinoma. Oncoimmunology 9: 1731943, 2020.
18. Livak KJ and Schmittgen TD: Analysis of relative gene expression data using real-time quantitative PCR and the 2(-Delta Delta C(T)) method. Methods 25: 402-408, 2001.
19. Hong W, Liang L, Gu Y, Qi Z, Qiu H, Yang X, Zeng W, Ma L and Xie J: Immune-related lncRNA to construct novel signature and predict the immune landscape of human hepatocellular carcinoma. Mol Ther Nucleic Acids 22: 937-947, 2020.
20. Zhao X, Liu X and Cui L: Development of a five-protein signature for predicting the prognosis of head and neck squamous cell carcinoma. Aging (Albany NY) 12: 19740-19755, 2020.
21. Dong HX, Wang R, Jin XY, Zeng J and Pan J: LncRNA DGCR5 promotes lung adenocarcinoma (LUAD) progression via inhibiting hsa-mir-22-3p. J Cell Physiol 233: 4126-4136, 2018.
22. Tian Y, Yu M, Sun L, Liu L, Wang J, Hui K, Nan Q, Nie X, Ren Y and Ren X: Distinct patterns of mRNA and lncRNA expression differences between lung squamous cell carcinoma and adenocarcinoma. J Comput Biol 27: 1067-1078, 2020.
23. Yang L, Wu Y, Xu H, Zhang J, Zheng X, Zhang L, Wang Y, Chen W and Wang K: Identification and validation of a novel six-lncRNA-based prognostic model for lung adenocarcinoma. Front Oncol 11: 775583, 2022.
24. Zhang H, Guo L and Chen J: Rationale for lung adenocarcinoma prevention and drug development based on molecular biology during carcinogenesis. Onco Targets Ther 13: 3085-3091, 2020.
25. Sun Q, Qin X, Zhao J, Gao T, Xu Y, Chen G, Bai G, Guo Z and Liu J: Cuproptosis-related LncRNA signatures as a prognostic model for head and neck squamous cell carcinoma. Apoptosis 28: 247-262, 2023.
26. Cao Q, Dong Z, Liu S, An G, Yan B and Lei L: Construction of a metastasis-associated ceRNA network reveals a prognostic signature in lung cancer. Cancer Cell Int 20: 208, 2020.
27. Zhang P, Pei S, Liu J, Zhang X, Feng Y, Gong Z, Zeng T, Li J and Wang W: Cuproptosis-related lncRNA signatures: Predicting prognosis and evaluating the tumor immune microenvironment in lung adenocarcinoma. Front Oncol 12: 1088931, 2022.
28. Bian M, Wang W, Song C, Pan L, Wu Y and Chen L: Autophagy-related genes predict the progression of periodontitis through the ceRNA network. J Inflamm Res 15: 1811-1824, 2022.
29. Wang G, Ye Q, Ning S, Yang Z, Chen Y, Zhang L, Huang Y, Xie F, Cheng X, Chi J, *et al*: LncRNA MEG3 promotes endoplasmic reticulum stress and suppresses proliferation and invasion of colorectal carcinoma cells through the MEG3/miR-103a-3p/PDHB ceRNA pathway. Neoplasma 68: 362-374, 2021.
30. Xuan J, Zhu D, Cheng Z, Qiu Y, Shao M, Yang Y, Zhai Q, Wang F and Qin F: Crocin inhibits the activation of mouse hepatic stellate cells via the lnc-LFAR1/MTF-1/GDNF pathway. Cell Cycle 19: 3480-3490, 2020.
31. Mafra ACP and Dias SMG: Several faces of glutaminase regulation in cells. Cancer Res 79: 1302-1304, 2019.
32. Wang T, Zhang XD and Hua KQ: A ceRNA network of BBOX1-AS1-hsa-miR-125b-5p/hsa-miR-125a-5p-CDKN2A shows prognostic value in cervical cancer. Taiwan J Obstet Gynecol 60: 253-261, 2021.
33. Liu J, Liu Q, Shen H, Liu Y, Wang Y, Wang G and Du J: Identification and validation of a three pyroptosis-related lncRNA signature for prognosis prediction in lung adenocarcinoma. Front Genet 13: 838624, 2022.
34. Sun X, Song J, Lu C, Sun X, Yue H, Bao H, Wang S and Zhong X: Characterization of cuproptosis-related lncRNA landscape for predicting the prognosis and aiding immunotherapy in lung adenocarcinoma patients. Am J Cancer Res 13: 778-801, 2023.
35. Zhang S, Li X, Tang C and Kuang W: Inflammation-related long non-coding RNA signature predicts the prognosis of gastric carcinoma. Front Genet 12: 736766, 2021.
36. Zhou D, Wang J and Liu X: Development of six immune-related lncRNA signature prognostic model for smoking-positive lung adenocarcinoma. J Clin Lab Anal 36: e24467, 2022.
37. Qiu Y, Yao J, Li L, Xiao M, Meng J, Huang X, Cai Y, Wen Z, Huang J, Zhu M, *et al*: Machine learning identifies ferroptosis-related genes as potential diagnostic biomarkers for osteoarthritis. Front Endocrinol (Lausanne) 14: 1198763, 2023.
38. Wang D, Tian Z, Zhang P, Zhen L, Meng Q, Sun B, Xu X, Jia T and Li S: The molecular mechanisms of cuproptosis and its relevance to cardiovascular disease. Biomed Pharmacother 163: 114830, 2023.
39. Wang F, Lin H, Su Q and Li C: Cuproptosis-related lncRNA predict prognosis and immune response of lung adenocarcinoma. World J Surg Oncol 20: 275, 2022.
40. Yalimaimaiti S, Liang X, Zhao H, Dou H, Liu W, Yang Y and Ning L: Establishment of a prognostic signature for lung adenocarcinoma using cuproptosis-related lncRNAs. BMC Bioinformatics 24: 81, 2023.
41. Zheng J, Zhao Z, Wan J, Guo M, Wang Y, Yang Z, Li Z, Ming L and Qin Z: N-6 methylation-related lncRNA is potential signature in lung adenocarcinoma and influences tumor microenvironment. J Clin Lab Anal 35: e23951, 2021.
42. Liu L, Wang T, Huang D and Song D: Comprehensive analysis of differentially expressed genes in clinically diagnosed irreversible pulpitis by multiplatform data integration using a robust rank aggregation approach. J Endod 47: 1365-1375, 2021.
43. Yang L, He YT, Dong S, Wei XW, Chen ZH, Zhang B, Chen WD, Yang XR, Wang F, Shang XM, *et al*: Single-cell transcriptome analysis revealed a suppressive tumor immune microenvironment in EGFR mutant lung adenocarcinoma. J Immunother Cancer 10: e003534, 2022.
44. Franzese O, Palermo B, Frisullo G, Panetta M, Campo G, D'Andrea D, Sperduti I, Taje R, Visca P and Nisticò P: ADA/CD26 axis increases intra-tumor PD-1$^{+}$CD28$^{+}$CD8$^{+}$ T-cell fitness and affects NSCLC prognosis and response to ICB. Oncoimmunology 13: 2371051, 2024.